ELECTROMECHANICAL SIMULATION AND TEST OF ROTATING SYSTEMS WITH MAGNETIC BEARING OR PIEZOELECTRIC ACTUATOR ACTIVE VIBRATION CONTROL

Alan B. Palazzolo, Punan Tang, Chaesil Kim, Daniel Manchala and Tim Barrett
Department of Mechanical Engineering, Texas A&M University
College Station, TX

Albert F. Kascak*, Gerald Brown, Gerald Montague** and Eliseo DiRusso
NASA Lewis
Cleveland, OH
* U.S. Army at Lewis, ** Sverdrup at Lewis

Steve Klusman
GMC Allison Gas Turbine
Indianapolis, IN

Reng Rong Lin
A.C. Compressor
Appleton, WI

ABSTRACT

This paper contains a summary of the experience of the authors in the field of electromechanical modeling for rotating machinery - active vibration control. Piezoelectric and magnetic bearing actuator based control are discussed.

INTRODUCTION

The stability analysis of conventionally supported rotating machinery has been treated extensively for many years. More recently attention has been focused on the stability analysis of magnetically supported flexible rotor or rotor-bearing installations with active vibration control systems. Assembling the model for this analysis has four basic steps:

(a) Form the passive mass, stiffness, damping model from the shaft and disc geometry and from the flow, fluid and geometric properties of bearings and seals;

(b) Obtain transfer function representation of all frequency dependent components in the feedback loop of the control system. This typically includes sensors, power amplifiers, digital signal processors and actuators;

(c) Assembly (coupling) of the frequency dependent component representations in (b) with the passive rotor-bearing-seal system model in (a);

(d) Solution of the characteristic equation of the closed loop system for the eigenvalues and inspection of the eigenvalues to investigate stability.

In a previous paper [1], the authors demonstrated how step (b) could be accomplished by curve fitting the component's frequency response to that of a 2nd order low pass electrical filter. This approach provided a 2nd order linear differential equation representation of the component which could be very easily coupled to the rotor system model to accomplish task (c). Task (d) was then performed utilizing the QR algorithm to extract the eigenvalues from the finite element formulated closed loop model.

Maslen and Bielk [2] presented an approach for coupling a frequency dependent, feedback loop component with a generically defined transfer function, to a standard finite element rotor system model. This method avoids the problems encountered in transfer matrix based approaches to solving the closed loop stability problem, namely non-collocated sensor-actuators and frequency dependent feedback components.

Ramesh and Kirk [3] presented a comparison between their F.E. approach to electromechanical system (ES) modeling and a transfer matrix based approach. Their results show good agreement between the methods; however, no analytical treatment of their F.E. approach was provided. Ku and Chen [4] present a F.E. based method for stability analysis of ES models and demonstrate it on our industrial pump model. The approach appears very accurate but it may be somewhat inefficient in that the eigenvalue problem must be solved repeatedly while making guesses at the natural frequencies.

This manuscript provides a review of the author's experience in electromechanical system modeling for this application. Theory and test results are given, along with a chronologically based description of the evaluation of the current modeling's methodology.

DISCUSSION

The test and theoretical results for piezoelectric actuator active vibration control are given in reference [5]. The test rig employed in that study is shown in Figure 1. The theoretical results in that paper assume ideal actuators, amplifiers and controllers which do not exhibit phase lag or amplitude roll off. Typical predicted unbalance response curves for various derivative feedback gains are shown in Figure 2. The governing equation for this system only represents pure proportional feedback gain (constant gain, zero phase lag) and pure derivative feedback gain (linear dependence of gain on frequency, 90° phase lead).

This simulation approach was improved in reference [1] where the actuator and amplifier's frequency response functions were represented by 2nd order low pass filters. Figures 3 and 4 show the measured and curve fit frequency response functions of a piezoelectric actuator. The curved fit representation represents 2nd

order differential equations which are assembled with the mechanical model to form a closed loop electromechanical model. Figures 5 and 6 show the shape of the measured and predicted unstable mode shapes for the same test rig as shown in Figure 1. Note that the frequency of that instability is approximately 2100-2400 Hz. The closed loop model was employed to investigate the effects of a 4th order low pass filter on stability of the unstable mode yielding the plots of Real (eigenvalue) versus feedback gain and cutoff frequency in Figure 7.

The authors [6] improved on this approach by employing a general order transfer function-state variable representation of any component in the feedback path. The approach is similar to [2]; however, a systematic method is provided for obtaining the transfer function from test data. A theory-test correlation is presented in this paper employing the test rig shown in Figures 8 and 9. This test rig was previously described in reference [7]. Figure 10 shows the measured and curve-fit 8th order transfer function through the summed proportional and derivative feedback paths of the digital controller. State space representations of this controller and the power amplifier were assembled along with a finite element model of the rotor (Figure 9) to predict the stability bounds of the coupled electromechanical system. Figure 11 shows a comparison between the predicted and measured stability boundaries in the proportional-derivative feedback gain space. Simulation results are shown for various values of a parameter that characterizes the back emf induced by vibrations of the shaft, as explained in reference [6].

Actuators and sensors are always mounted on a support structure with some flexibility and inertia of its own. Reference [7] describes a simulation study for closed loop stability including effects of actuator and sensor mount flexibility. The rotor model was the same one as employed in references [1] and [5], and is depicted in Figure 12. The casing was simulated with 9 node, isoparametric thick shell elements and the actuators and sensors were attached to the flexible casing. Figures 13 and 14 are typical of results shown in reference [7]. Note how one of the three unstable modes shown in Figure 13 for the case of sensor mounted to casing does not appear if the sensor mount is assumed to be rigid as shown in Figure 14.

Figure 15 depicts a current research test being conducted by the authors for predicting stability bounds for a gas turbine engine simulator. This installation employs a PID based digital controller, pulse width modulated power amplifier and a high temperature magnetic bearing. Figure 16 shows the measured and curve fit transfer function through the summed proportional and derivative paths of the controller. The measured and predicted stability bounds will be determined and published in the near future.

SUMMARY

This manuscript summarizes the authors' efforts in the area of active vibration control related—electromechanical system modeling. Initial efforts employed ideal feedback component characterizations that were free of rolloff and phase lag. The later research of the authors utilized more realistic models based on transfer functions through the feedback components. The future work in this area will concentrate on additional test verifications of the method.

ACKNOWLEDGMENTS

Sincere gratitude is extended to the Dynamics Branch at NASA Lewis, the U.S. Army at NASA Lewis and the Texas A&M Turbomachinery Consortium (TRC) for funding this work. Appreciation is also extended to Allison Gas Turbine for their participation in this NASA/Industry/University cooperative work program.

REFERENCES

1. Lin, Reng Rong and Palazzolo, A.B., "Electromechanical Simulation and Testing of Actively Controlled Rotordynamic Systems with Piezoelectric Actuators," *Trans. ASME Journal of Gas Turbines and Power*, Vol. 115, April, 1993, pp. 324-335.

2. Maslen, E.H. and Bielk,J.R., "Implementing Magnetic Bearing in Discrete Flexible Structure Models," submitted to *Trans. ASME Journal of Dynamics and Controls,* 1991.

3. Ramesh, K. and Kirk, R.G., "Subharmonic Resonance Stability Prediction for Turbomachinery with Active Magnetic Bearings," *Proceedings of the Third International Symposium on Magnetic Bearings*, Alexandria, Virginia, July, pp. 113-122.

4. Ku, C.-P.R. and Chen, H.M., "An Efficient Method for Stability Analysis for Active Magnetic Bearing System," *Proceedings of the Third International Symposium on Magnetic Bearings*, Alexandria, Virginia, July, pp. 133-142.

5. Palazzolo, A.B., et. al, "Test and Theory for Piezoelectric Actuator - Active Vibration Control of Rotating Machinery," *ASME Journal of Vibrations and Acoustics*, April, Vol. 113, 1991, pp. 167-175.

6. Tang, P., Palazzolo, A.B., Brown, G., DiRusso, E. and Kascak, A., *International Gas Turbine Conference ASME*, 5/24-5/27, 1993, paper no. 93-GT-382.

7. Barrett, T., Palazzolo, A.B. and Kascak, A.F., *International Gas Turbine Conference ASME*, 5/24-5/27, 1993, paper no. 93-GT-293

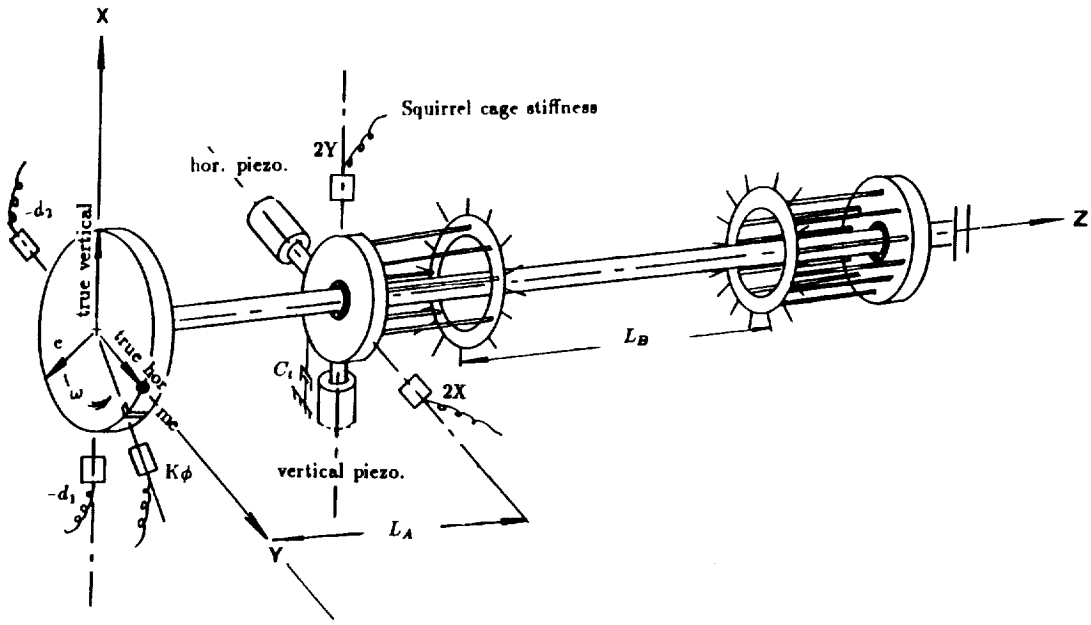

Figure 1. Diagram of test rig with Piezoelectric pushers.

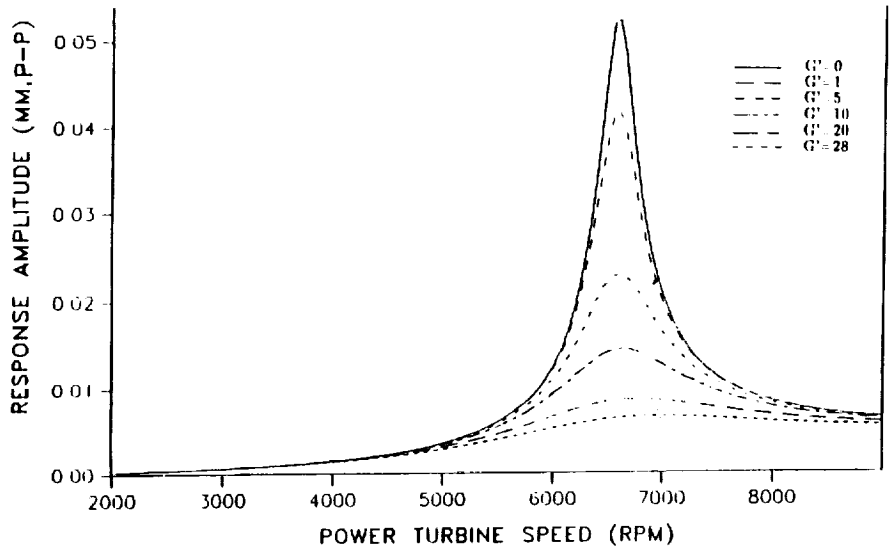

Figure 2. Simulation unbalance response at probe 2X or 2Y
vs. feedback gain coefficients in ADFT.

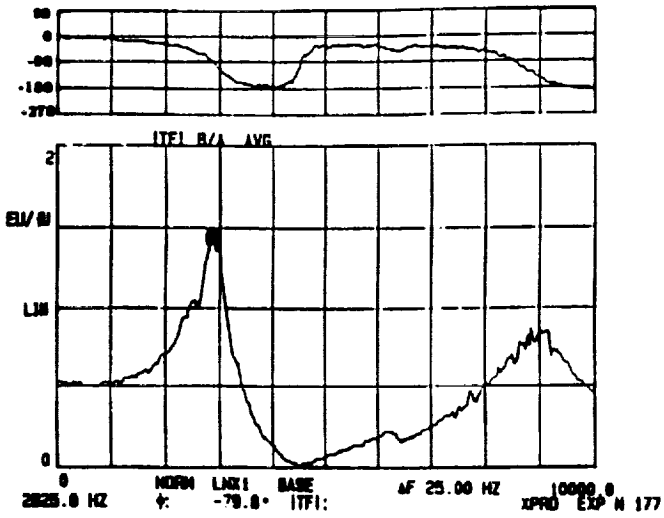

Figure 3. Transfer function plot of a typical pusher.

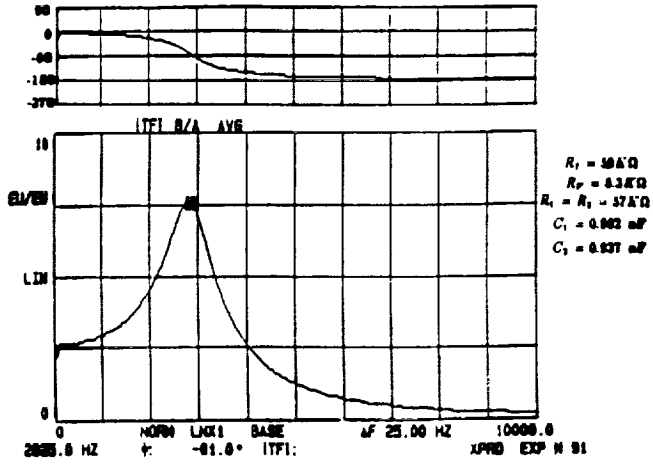

Figure 4. Transfer function plot of realized electrical circuit of pusher A.

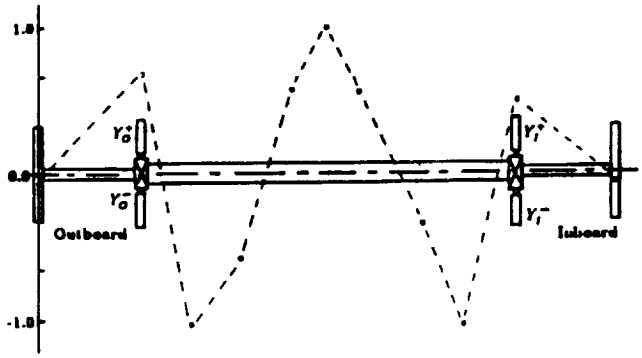

Figure 5. Measured mode shape of unstable mode at a frequency of 2100 Hz.

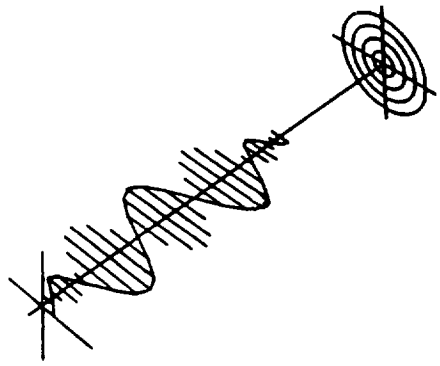

Figure 6. Predicted mode shape of unstable mode at 2400 Hz.

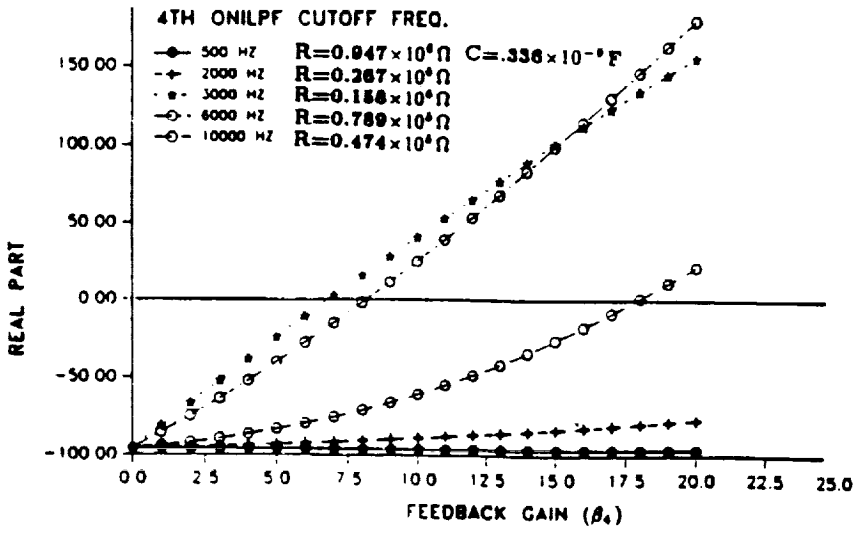

Figure 7. Effects of cutoff frequency of 4NILPF on the system instability onset gain.

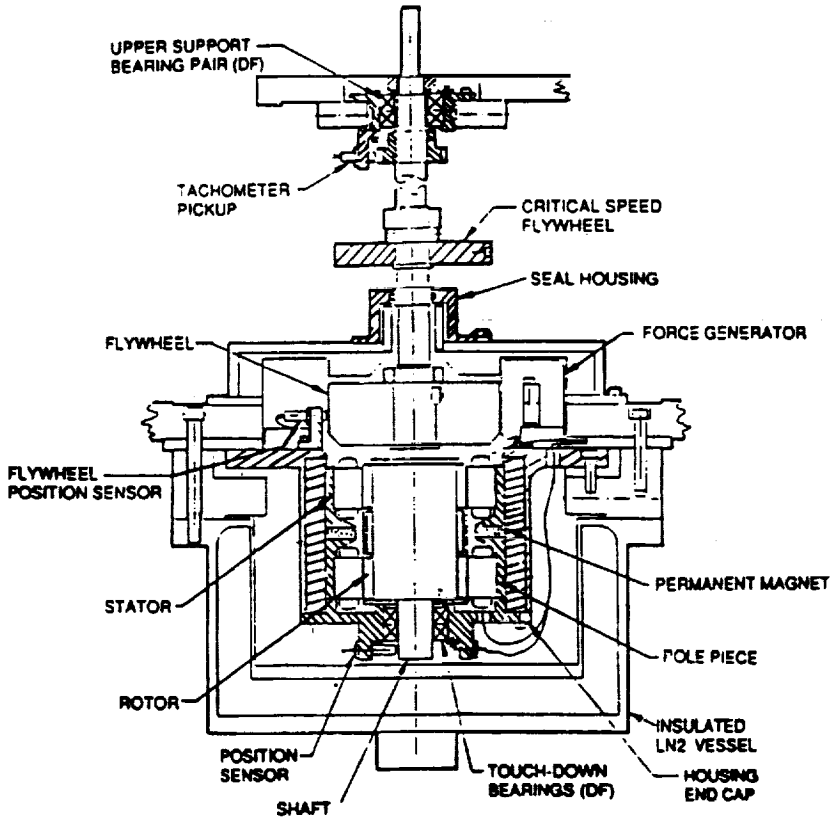

Figure 8. Cryogenic Magnetic Bearing Test Facility Design.

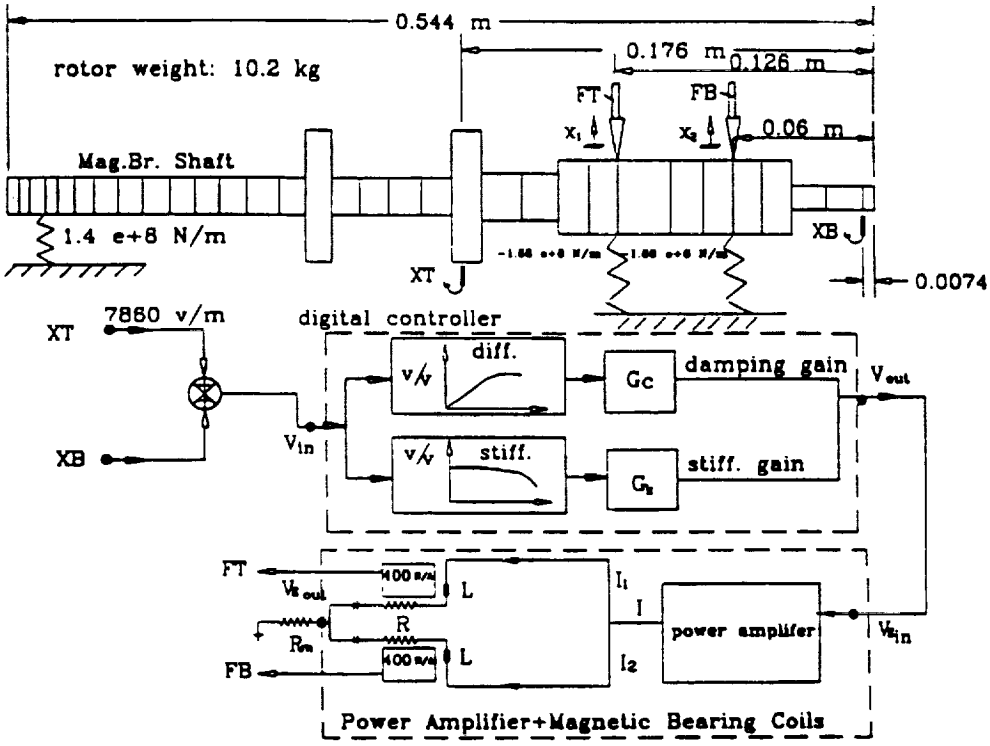

Figure 9. Block Diagram of rotor controller and magnetic bearing.

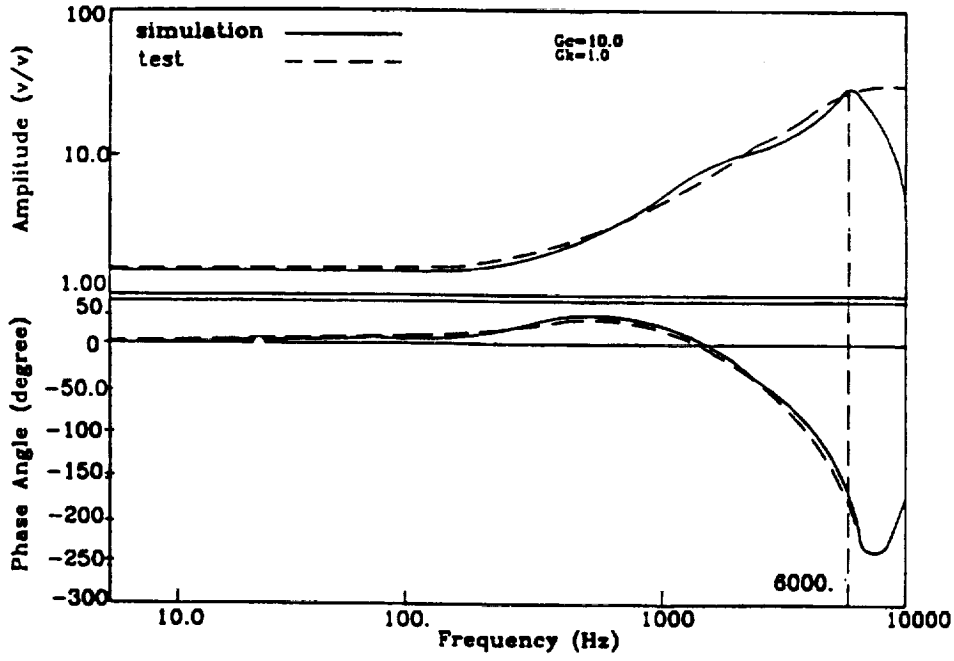

Figure 10. Measured and Curve Fit frequency response function for DSP.

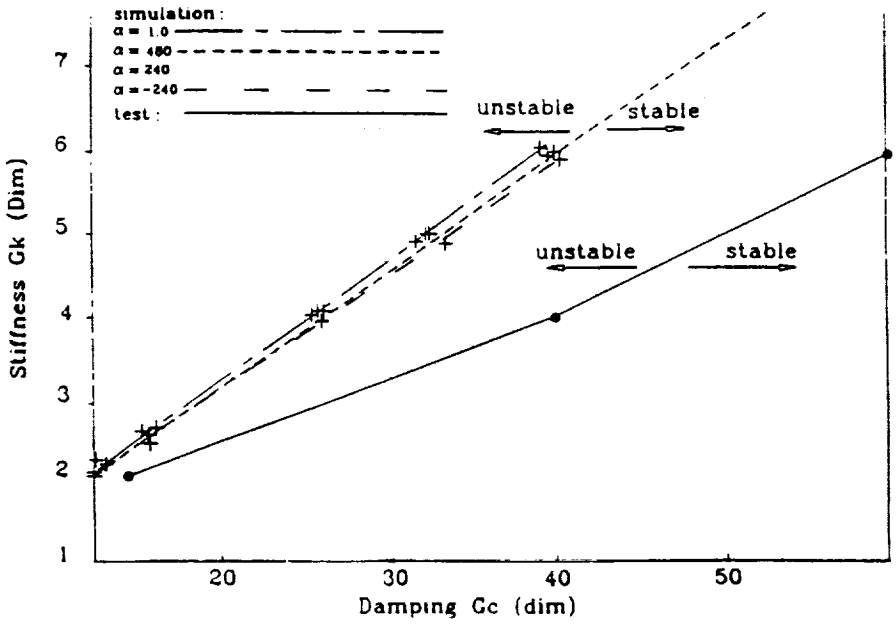

Figure 11. Comparison of measured and predicted natural frequencies on the instability threshold.

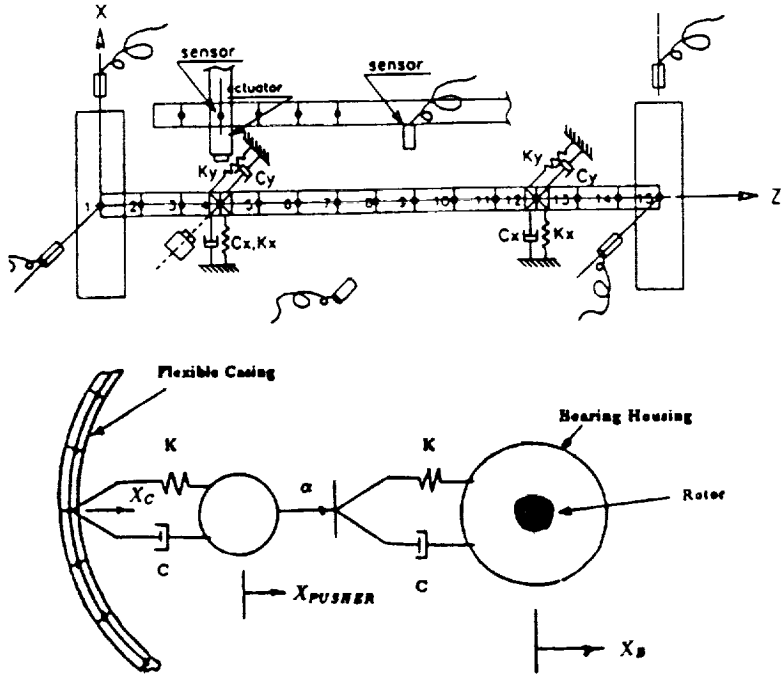

Figure 12. Fourteen mass rotor model and actuator connection.

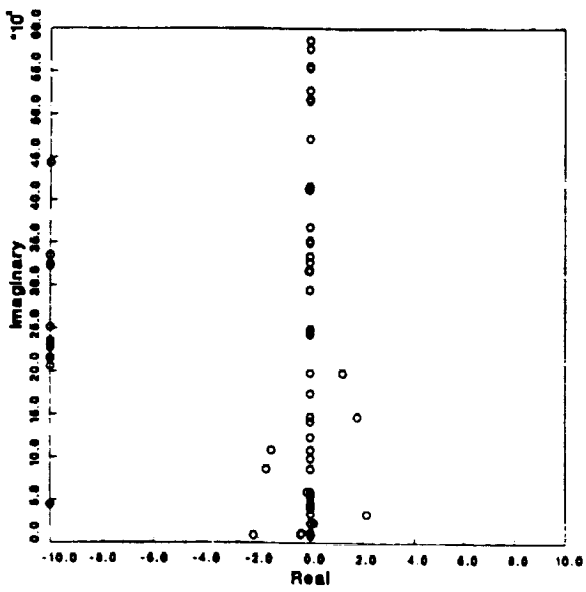

Figure 13. 1/16" casing wall thickness eigenvalue stability graph.

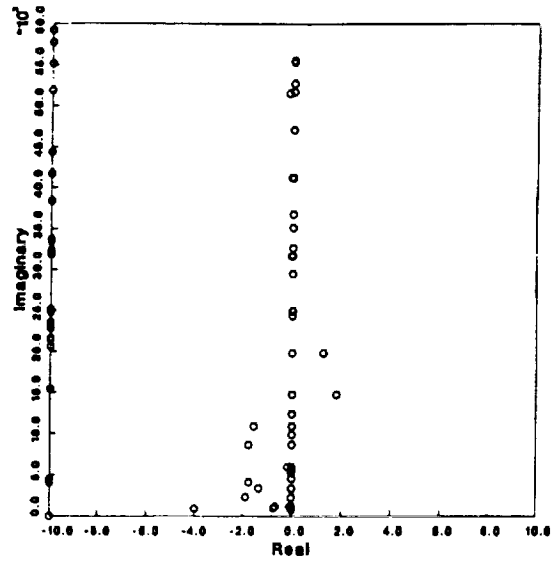

Figure 14. Uncoupled sensor - (1/16" casing).

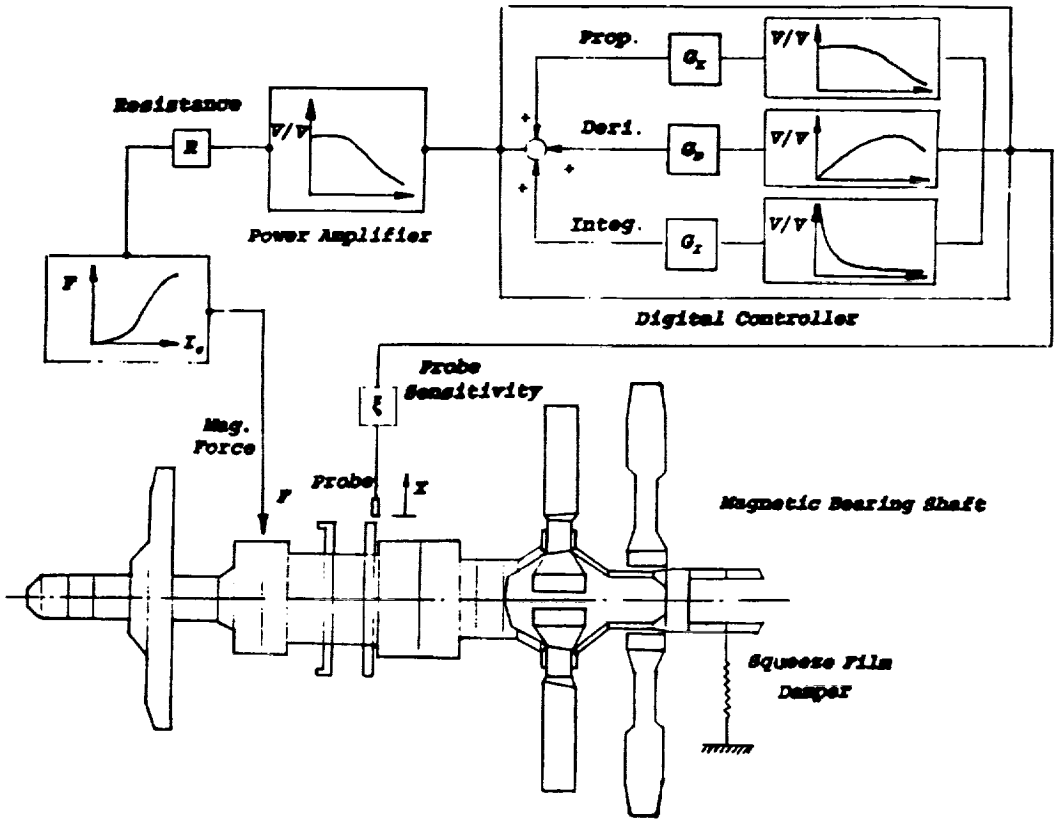

Figure 15. Block diagram of industrial magnetic bearing rotor.

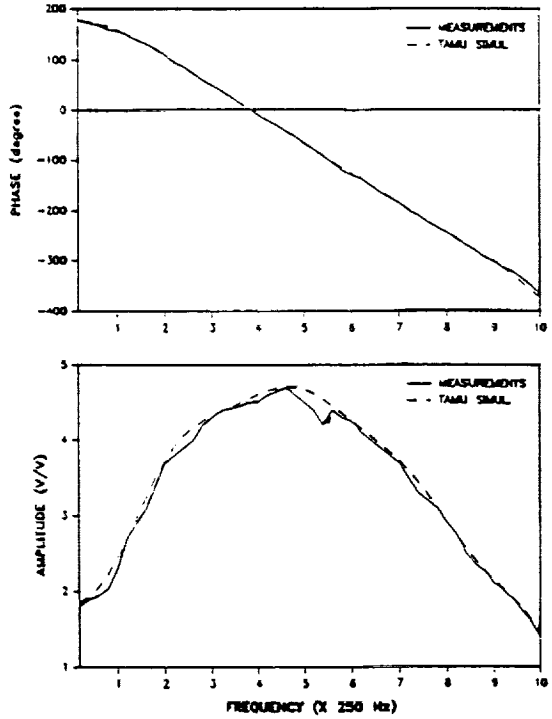

Figure 16. Comparison of TAMU simulation and Measurement (p:-10 and D:-50).